Visual
Abstract

Fatigue crack growth simulation of two non-coplanar embedded cracks using s-version finite element method

Akiyuki Takahashi, Ayaka Suzuki, Masanori Kikuchi
Tokyo University of Science, Japan
takahash@rs.noda.tus.ac.jp, 7516629@ed.tus.ac.jp, kik@rs.noda.tus.ac.jp

ABSTRACT. In this paper, the fatigue crack growth simulation of two non-coplanar embedded cracks using the s-version finite element method is presented, and the validity and reliability of the alignment rule for two non-coplanar cracks are evaluated. According to the previous numerical and experimental studies on two non-coplanar surface cracks, the simulated fatigue crack growth behavior is categorized into five patterns to discuss the criteria for the application of the alignment rule. The results suggest that the strength of interaction between the non-coplanar embedded cracks is similar to that between non-coplanar surface cracks. Finally, the interaction of the cracks is evaluated by the stress intensity factor, and the categorization of the fatigue crack growth behavior is discussed by the stress intensity factor. It can be found that the boundary corresponding to the criteria of the application of the alignment rule can be determined as the ratio of the stress intensity factor is 4%. Thus, instead of making a decision of the fatigue crack growth pattern based on the visual inspection, the ratio of the stress intensity factor can be used, and should give more quantitative evaluation of the interaction of two non-coplanar embedded cracks.

KEYWORDS. Non-coplanar embedded cracks; Fatigue crack growth; Stress intensity factor; Alignment rule; S-version finite element method.

OPEN ACCESS

INTRODUCTION

Fatigue crack growth is a classical but critical issue to ensure the structural reliability. Up till now, many experimental and numerical studies on the fatigue crack growth of surface cracks have been conducted to model the complex behavior of fatigue crack growth and establish an accurate evaluation method of the residual fatigue life [1-3]. In the fitness-for service (FFS) code for nuclear power plants, flaws detected in structural components are assumed to be simple elliptical cracks and are evaluated using well-established stress intensity factor calculation methods for the simple elliptical cracks [4]. If two non-coplanar cracks appear and are detected in their close vicinity, according to the alignment rule in the FFS code, one of the cracks is projected onto the plane of the other crack. Furthermore, if the projected crack touches or overlaps with the other crack, the cracks are combined into a simple elliptical crack. The combination of cracks is controlled

by the combination rule in the FFS code. The stress intensity factor calculation methods in the FFS code can then be applicable to the simple elliptical cracks. Therefore, the validity and reliability of the alignment and combination rules are of great interest to ensure the appropriate assessment of the structural integrity. In order to evaluate the validity and reliability of the alignment and combination rules, it is necessary to check the fatigue crack growth behavior and the interaction of the non-coplanar cracks.

Owing to the development of computers and computer simulation techniques, computer simulation is now a powerful approach to complex crack growth problems. Kamaya et al. has applied the s-version finite element method (s-FEM) to fatigue crack growth simulations, and successfully simulated complex fatigue crack growth behavior [5]. Using the s-FEM, the cracks are modelled by local meshes. The local meshes are then superimposed onto a global mesh, which models the geometry and boundary conditions of the structure of interest. The global and local meshes can be separately modelled so that the complexity in the mesh generation of cracked structures can be drastically reduced. This remarkable property of s-FEM in the mesh generation process is a great advantage in the fatigue crack growth simulation, where the finite element meshes must be repeatedly remodeled in accordance with the updated crack shape.

In this paper, the fatigue crack growth simulation of two non-coplanar embedded cracks using the s-FEM is presented, and the validity and reliability of the alignment rule for two non-coplanar cracks are evaluated. According to the previous numerical and experimental studies on two non-coplanar surface cracks [6], the simulated fatigue crack growth behavior is categorized into five patterns to discuss the criteria for the application of the alignment rule. Finally, the interaction of the cracks is evaluated by the stress intensity factor, and the categorization of the fatigue crack growth behavior is discussed in terms of the stress intensity factor.

COMPUTATIONAL METHOD

In this study, the fatigue crack growth behavior of two non-coplanar cracks are simulated using the s-FEM. In the s-FEM, as shown in Fig. 1, the geometry and boundary conditions of structures are modeled with a global mesh. Cracks are modeled with local meshes separately from the global mesh, and can be inserted into the structures by superimposing the local meshes on the global mesh. The displacement functions of the global and local meshes are independently defined. As an example, if the structure has two cracks, the problem is modelled with a global mesh and two local meshes for each crack. The displacement function for the global mesh is defined as $u_i^G(x)$, and for the local meshes, $u_i^{L1}(x)$ and $u_i^{L2}(x)$. By superimposing the displacement functions, the displacement field of the structure is defined as

$$u_i(x) = \begin{cases} u_i^G(x) & x \in \Omega^G - \left(\Omega^{L1} + \Omega^{L2} - \Omega^I \right) \\ u_i^G(x) + u_i^{L1}(x) & x \in \Omega^G - \Omega^I \\ u_i^G(x) + u_i^{L2}(x) & x \in \Omega^G - \Omega^I \\ u_i^G(x) + u_i^{L1}(x) + u_i^{L2}(x) & x \in \Omega^I \end{cases} \tag{1}$$

where, Ω^G is the entire volume of the structure, Ω^{L1} and Ω^{L2} are for the volumes defined by the local meshes, and Ω^I is the volume overlapped with the local meshes. In order to preserve the continuity of the displacement function at the boundaries of local meshes, the displacement at the boundaries of the local meshes are fully constraint. Thus, the displacement can be equal to the displacement of global mesh. The displacement equation can then be calculated in accordance with the definition of displacement function given in Eqn. (1). The detailed information about the s-FEM can be found elsewhere [7].

Since the local meshes can be modelled separately from the global mesh, the complex shape of cracks can be easily modelled in the s-FEM. Thus, due to the remarkable advantage of the s-FEM in the modeling of cracks, the fatigue crack growth simulation, where the finite element mesh for cracks must be repeatedly updated, can be performed easily by the s-FEM. In our developed fatigue crack growth simulation system, the crack front shape is modelled with a number of segments, and the local meshes are automatically modeled using the segment data. The global mesh is prepared only at the beginning of the simulation, and is used repeatedly for the entire simulation. The energy release rate along the crack tip is calculated by the virtual crack closure method (VCCM) [8]. The energy release rate calculated by the VCCM is simply converted into the stress intensity factor. Then, the stress intensity factor range is calculated with the stress intensity factor and the stress ratio. Using the stress intensity factor range, the crack growth amount and direction are then determined by the Paris law [9] and

the criteria proposed by Richard et al. [10]. The positions of crack tip segments are updated in accordance with the calculated crack growth amount and direction.
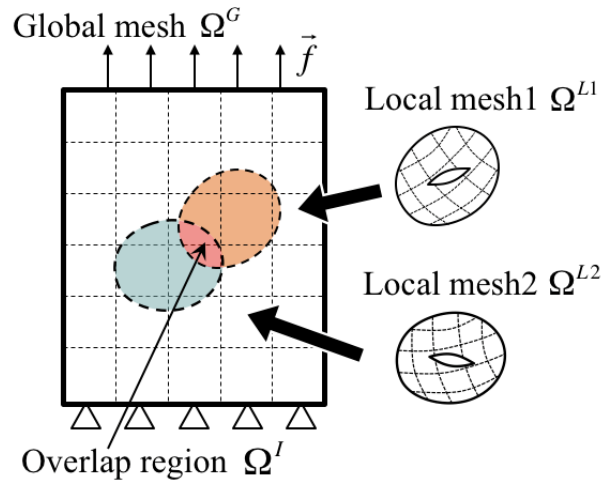

Figure 1: A schematics of the s-FEM. The geometry and boundary conditions are modeled with global mesh. The cracks are modeled with local meshes separately from the global mesh. The local meshes are superimposed on the global mesh to obtain the displacement solution of the problem.
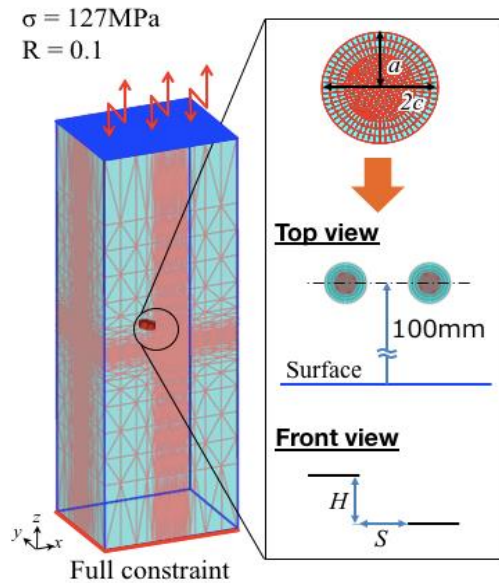

Figure 2: Finite element mesh for the fatigue crack growth simulation of two non-coplanar embedded cracks. Each cracks is modelled with each local mesh separately. The position of the center of two cracks are at 100 mm distance from the surface of the specimen. The horizontal separation and vertical height of the crack tips are denoted by H and S. The maximum tensile stress is 127 MPa, and the stress ratio R is 0.1. The displacement at the bottom surface is fully constraint.

FATIGUE CRACK GROWTH SIMULATION OF TWO NON-COPLANAR EMBEDDED CRACKS

In this paper, we focus on the validity and reliability of the alignment rule in the FFS code, the fatigue crack growth behavior of two non-coplanar embedded cracks are simulated. Fig. 2 shows the finite element model of the fatigue crack growth simulation of two non-coplanar embedded cracks. Two circular embedded cracks are embedded in a rectangular shape of specimen. The size of the rectangular specimen in x, y and z direction are 750 mm, 250 mm and 200 mm, respectively. The center of two cracks are located at 100 mm distance from the surface of the specimen, and the cracks

are aligned parallel to the surface. The rectangular shape of the specimen is modeled with a global mesh. 10-noded tetrahedral elements are used for the global mesh. The numbers of elements and nodes are 115,200 and 171,245, respectively. On the other hand, the two cracks are modeled with two local meshes separately. 20-noded hexahedral elements are used for the local meshes. The initial numbers of elements are nodes are 13,680 and 61,210, respectively. The half-depth and length of crack is denoted by a and c. The initial horizontal and vertical distance of the two cracks are denoted by S and H. In the FFS code, the alignment rule is compiled with the horizontal and vertical distance of two cracks, the horizontal and vertical distance are changed to study how the two cracks grow under cyclic loading. The maximum tensile stress of the cyclic loading is assumed to be 127 MPa, and the stress ratio R is set to 0.1. The tensile stress is applied to the finite element model by giving corresponding traction to the top surface of the specimen. The displacement of the bottom surface is fully constraint. The material is assumed to be a steel, and 1.67×10^{-12} and 3.23 are used as the coefficient and exponent of the Paris law [5]. In the Paris law, the units of stress intensity factor range ΔK and crack growth rate da/dN are MPamm$^{0.5}$ and m/cycle, respectively.

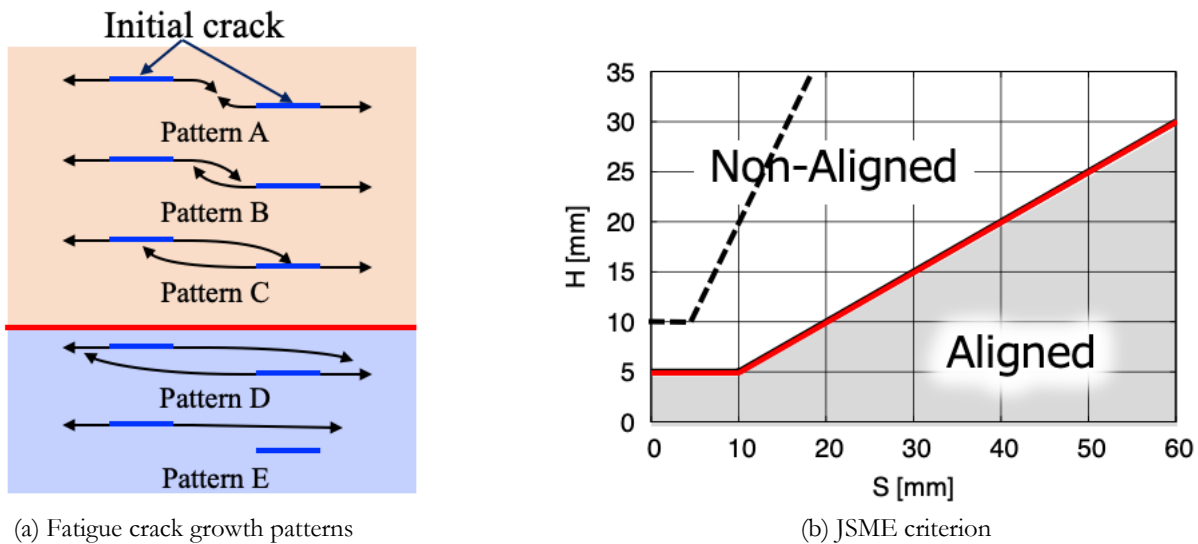(a) Fatigue crack growth patterns   (b) JSME criterion

Figure 3: (a) Fatigue crack growth patterns of two non-coplanar cracks and (b) the alignment rule given by the Japan Society for Mechanical Engineers (JSME). The red bold line in the right figure is determined by the experiments of the fatigue crack growth of surface cracks. Finite element mesh for the fatigue crack growth simulation of two non-coplanar embedded cracks. Each crack. The alignment rule is defined by the horizontal separation S and the vertical height H. The JSME criterion fully covers the area defined by the bold red line.

Ando et al. performed experiments of the fatigue crack growth of surface cracks, and categorized the fatigue crack growth behavior into five patterns as shown in Fig. 3 [3]. In the pattern A, the crack tips meet each other, and the cracks are naturally combined. In the pattern B, the crack tip direction is within the spacing between the initial crack tips. In the pattern C, the crack tips go to the initial crack. In the pattern D, the crack tips pass the initial cracks. In the pattern E, only one of cracks grows horizontally, and never meet the other crack. Ando et al. determined that the alignment rule must be applied if the fatigue crack growth behavior is patterns A, B and C [3]. The border of the application and non-application of the alignment rule shown in Fig. 3 with the bold red line is obtained by the experiments of surface cracks; therefore, in order to clarify the applicability of the alignment rule to embedded cracks, the fatigue crack growth behavior of two non-coplanar embedded cracks must be observed, and the crack growth behavior must be categorized into the five patterns.

The fatigue crack growth behavior of two non-coplanar embedded cracks is simulated. The crack size is fixed to a=2.5 mm and c=2.5 mm. The initial crack tip distance parameters S and H are changed in a range from 2.5 mm to 25 mm. The fatigue crack growth behaviors obtained by the s-FEM simulations for S=10 mm are shown in Fig. 4. Because the location of the two cracks is non-coplanar, the fatigue crack growth behavior is also non-planar, and the s-FEM simulation technique successfully reproduces such a complex fatigue crack growth behavior. The fatigue crack growth behaviors can be categorized into pattern B, C and D as shown in the figure. Fig. 5 shows the interaction map of the two non-coplanar embedded cracks obtained by the s-FEM simulations. Ando et al. discussed about the criteria of the application of the alignment rule based on the experiments of the fatigue crack growth of surface crack. The border of the application

determined by Ando et al. almost coincides with the boundary between the pattern C and D obtained by the s-FEM simulations. The results suggest that the strength of interaction between the non-coplanar embedded cracks is similar to that between non-coplanar surface cracks. Therefore, the alignment rule given by JSME can still give a conservative evaluation of not only surface cracks and also embedded cracks.
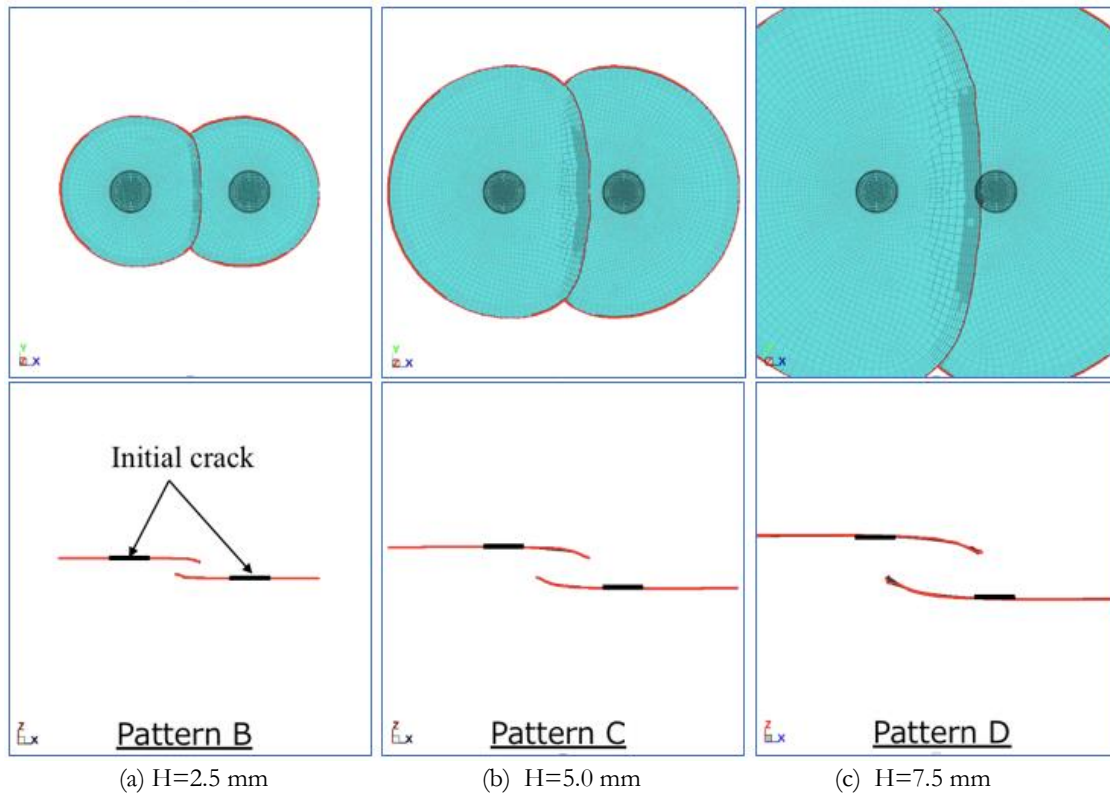

(a) H=2.5 mm (b) H=5.0 mm (c) H=7.5 mm

Figure 4: Fatigue crack growth behavior of two non-coplanar embedded cracks. The horizontal separation S of the initial crack tips is 10 mm, and the vertical height H is (a) 2.5 mm, (b) 5.0 mm and (c) 7.5 mm. Only crack shape is displayed. The red line shows the crack tip. The top figure is the top view of the crack shape, and the bottom figure is the front view of the crack shape. The crack growth behavior is categorized into (a) pattern B, (b) pattern C, and (c) pattern D, respectively.
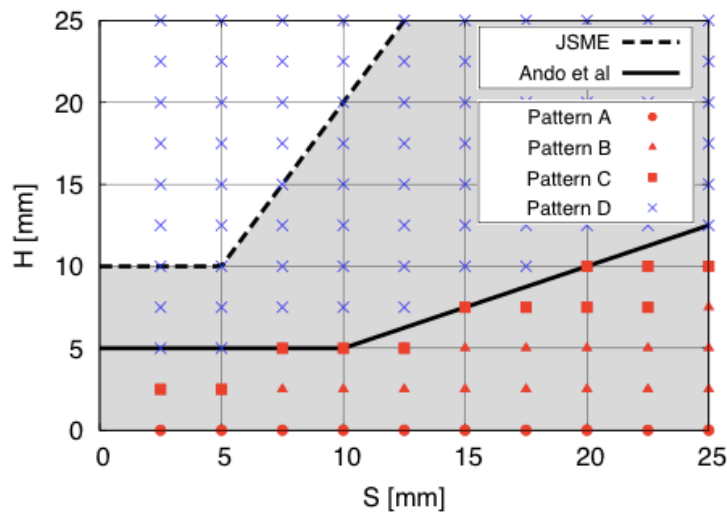

Figure 5: Interaction map of two non-coplanar embedded cracks obtained by the s-FEM simulations. The marks shows the fatigue crack growth patterns. The borders determined by the JSME and Ando et al. are also plotted.

As shown in Fig. 3 and 5, the alignment rule in the FFS code is established with the horizontal and vertical distance of two non-coplanar cracks. However, the unit of the horizontal and vertical distance is defined as mm. Therefore, there is a question on the validity of the application of the alignment rule to the other size of cracks. To check if it is valid to apply the same alignment rule to the other size of cracks, fatigue crack growth simulations of two non-coplanar cracks of $2c$=10 mm with various horizontal and vertical distances are performed. The results are shown in Fig. 6. In the figure, the solid and dotted lines are taken from respectively the JSME FFS code and experimental data obtained by Ando et al. [3]. In Fig. 5 where the crack size is $2c$=5 mm, the numerical results are fully covered by the dotted line taken from the experimental data. However, in Fig. 6, the some of the numerical results are over the dotted line. Therefore, the categorization of the fatigue crack growth behavior of two non-coplanar cracks has a dependence on the initial crack size. Thus, the alignment rule is not applicable to arbitrary size of embedded cracks. To remove the dependence of the categorization on the initial crack size shown in Fig. 6, the horizontal and vertical distance of two non-coplanar cracks are normalized by the half of the initial crack size c. The result is shown in Fig. 7. As a result of the normalization of the horizontal and vertical distances by the half of the initial crack size, the categorizations of the fatigue crack growth behavior of two non-coplanar cracks with $2c$=5 mm and 10 mm become almost identical. Thus, the results suggest that the horizontal and vertical distance of two non-coplanar cracks should be normalized by the initial crack size to apply the alignment rule to arbitrary size of cracks.
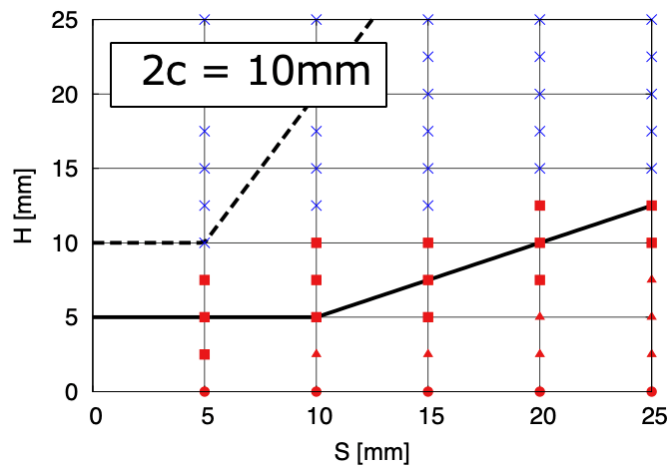

Figure 6: Interaction map of two non-coplanar embedded cracks obtained by the s-FEM simulations. The initial crack size is $2c$=10mm. The plot is based on the real length of H and S. The borders determined by the JSME and Ando et al. are also plotted.
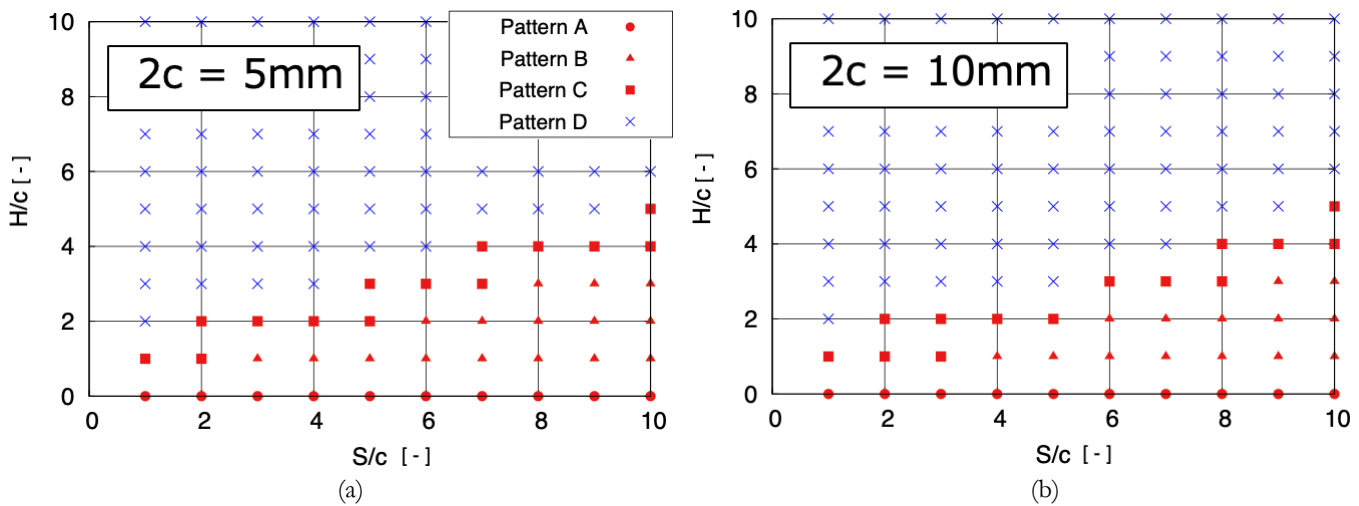

Figure 7: Interaction map of two non-coplanar embedded cracks obtained by the s-FEM simulations. The initial crack sizes are (a) $2c$=5mm and (b) $2c$=10mm. The plot is based on the length of H and S normalized by the half size of crack c. The borders determined by the JSME and Ando et al. are also plotted.

The categorization of the fatigue crack growth behavior and the discussion on the application of the alignment rule, in this study, is based on the visual inspection. In order to evaluate and discuss the alignment rule, the stress intensity factor of two non-coplanar embedded cracks is examined. As shown in Fig. 8, the stress intensity factor of two circular cracks is calculated. In the calculation, the horizontal separation of crack tips is zero. In order to investigate the interaction of the cracks, the stress intensity factor of a single crack with the same shape is also calculated. Fig. 8 shows an example of the stress intensity factor distribution along the crack tips. The stress intensity factor near the other crack increases as a result of the interaction. Comparing the stress intensity factor of two non-coplanar embedded cracks with that of the single crack, the strength of interaction is represented as the ratio of the maximum stress intensity factor increase to the stress intensity factor of the single crack. Fig. 9 shows the interaction map with the ratio. As shown in the figure, the boundary between the pattern B and C can be determined as the ratio of the stress intensity factor is 10%. On the other hand, as for the boundary between the pattern C and D, which is the criteria of the application of the alignment rule, the boundary can be determined as the ratio of the stress intensity factor is 4%. Thus, instead of making a decision of the fatigue crack growth pattern based on the visual inspection, the ratio of the stress intensity factor can be used, and should give more quantitative evaluation of the interaction of two non-coplanar embedded cracks.
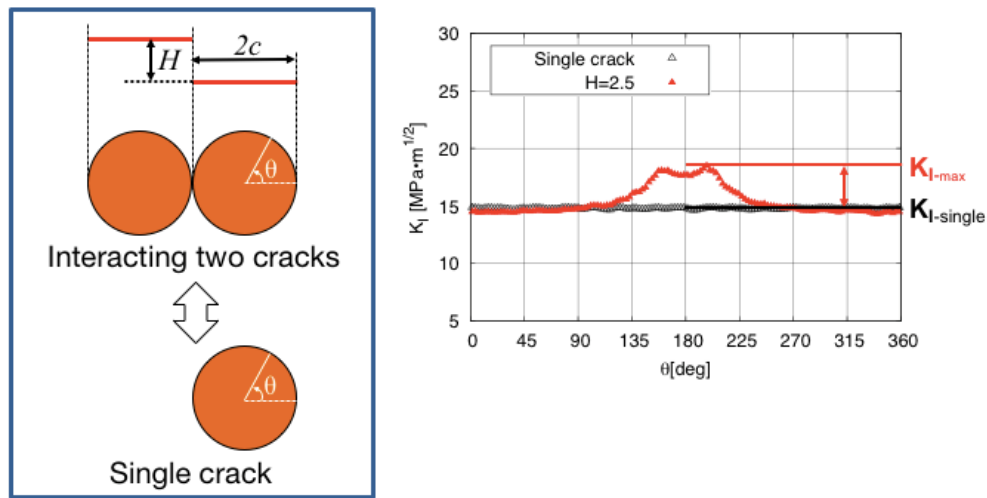

Figure 8: Stress intensity factor distribution along the crack tip of two non-coplanar embedded cracks. The stress intensity factor increases near the other crack. The position along the crack tip is denoted with the angle theta defined in the figure (left). In order to study the interaction of two embedded cracks, the stress intensity factor of a single embedded crack is also calculated.
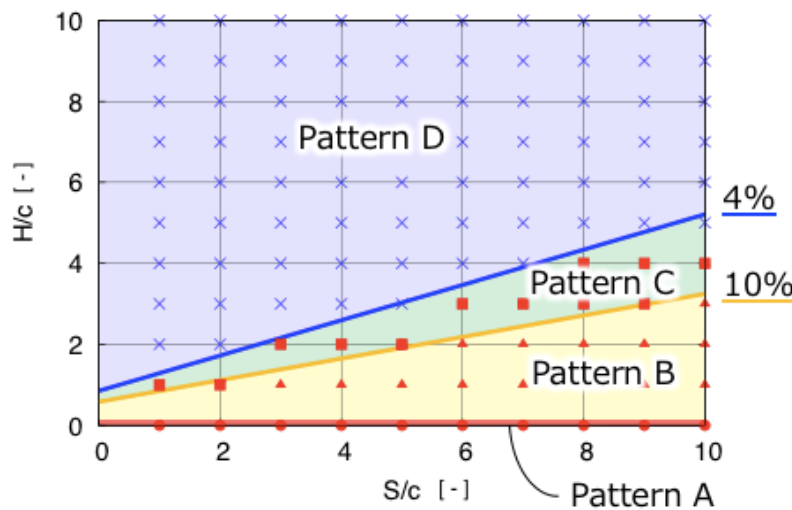

Figure 9: Interaction map of two non-coplanar embedded cracks. The value written in the left side of the figure shows the ratio of the maximum stress intensity factor of two non-coplanar embedded cracks to the stress intensity factor of the single crack. The horizontal and vertical axis of the figure is normalized by the initial half-length of the crack.

Conclusions

Fatigue crack growth simulations of two non-coplanar embedded cracks are performed using the s-FEM, and the fatigue crack growth behavior is evaluated by the visual inspection and the ratio of stress intensity factor. The s-FEM has a great advantage in the fatigue crack growth simulation, because the cracks can be modelled as local meshes separately from the global mesh, which is for the geometry and boundary conditions of structures. Using the s-FEM, the fatigue crack growth simulation could be performed automatically. We need to prepare only the global mesh and the crack front information, which is the number of segments along the crack tip. The complex non-planar behavior of two non-coplanar embedded cracks could be simulated with the s-FEM. Then, the fatigue crack growth behavior was categorized into five patterns to discuss the similarity of the fatigue crack growth behavior of embedded cracks and that of surface cracks. The results suggest that the location and shape of the boundary between the pattern C and D, which corresponds to the criteria for the application of the alignment rule, is very similar to those for the surface cracks. Therefore, the existing alignment rule is applicable to the embedded cracks, although the rule is established based on the numerical and experimental results of surface cracks. However, because the horizontal and vertical distance of two cracks are described with a mm unit, the alignment rule gives different results to different initial size of cracks. To remove the dependence of the alignment rule on the initial crack size, the horizontal and vertical distance of two cracks should be normalized by the half size of initial crack. Finally, the stress intensity factor of two non-coplanar embedded cracks and single cracks is calculated. Then, it could be found that the ratio of the maximum stress intensity factor of two non-coplanar embedded cracks to the stress intensity factor of the single crack can be a parameter to determine the fatigue crack growth pattern and the criteria for the application of the alignment rule.

References

[1] Brighenti R., Carpinteri A. (2013). Surface cracks in fatigued structural components: a review, Fatigue Frac. Eng. Mat. Struct., 36, pp. 1209-1222.

[2] Rozumek D., Faszynka S. (2017). Fatigue crack growth in 2017A-T4 alloy subjected to proportional bending with torsion, Frattura ed Integrità Strutturale, 42, pp. 23-29

[3] Sniezek L, Slezak T, Grzelak K, Hutsaylyuk V. (2016). An experimental investigation of propagation the semi-elliptical surface cracks in an austenitic steel. Int. J. Pressure Vessels and Piping, 144, pp. 35–44.

[4] Codes for Nuclear Power Generation Facilities, Rules on Fitness-for-Service for Nuclear Power Plants, JSME, (2016).

[5] Kamaya, M., Miyokawa, M., Kikuchi, M. (2010). Growth prediction of interacting surface cracks of dissimilar sizes, Eng. Frac. Mech., 77, pp. 3120-3131.

[6] Ando, K., Hirata, T., Iida, K. (1983). An Evaluation Technique for Fatigue Life of Multiple Surface Cracks: Part 2: A Problem of Multiple Parallel Surface Cracks, J. Marine Sci. Tech., (in Japanese), 153, pp. 352-363.

[7] Fish, J., Markolefas, S., Guttal, R., Nayak, P. (1994). On adaptive multilevel superposition of finite element meshes, Appl. Numer. Math., 14, pp. 135-164.

[8] Okada, H., Higashi, M., Kikuchi, M., Fukui, Y., Kumazawa, N. (2005). Three dimensional virtual crack closure-integral method (VCCM) with skewed and non-symmetric mesh arrangement at the crack front, Eng. Frac. Mech., 72, pp. 1717-1737.

[9] Paris, P., Erdogan, F. (1963). A Critical Analysis of Crack Propagation Laws, J. Basic Eng., Trans. American Society of Mechanical Engineers, pp. 528-534

[10] Richard, H.A., Fulland, M., Sander, M. (2005). Theoretical crack path prediction, Fatigue & Frac. Eng. Mater. Sci. 28, pp. 3-12.